Preprints, 22th Conf. on Weather Analysis and Forecasting
and 18th Conf. on Numerical Weather Prediction
Amer. Meteor. Soc., Park City, UT, 25-29 June 2007

10B.2 IMPACT OF MULTI-MOMENT MICROPHYSICS AND MODEL RESOLUTION ON PREDICTED COLD POOL AND REFLECTIVITY INTENSITY AND STRUCTURES IN THE OKLAHOMA TORNADIC SUPERCELL STORMS OF 3 MAY 1999

Daniel T. Dawson II*[1,2], Ming Xue[1,2], Jason A. Milbrandt[2], M. K. Yau[3], and Guifu Zhang[2]

[1]Center for the Analysis and Prediction of Storms and [2]School of Meteorology
University of Oklahoma, Norman, OK 73019
[2]Department of Atmospheric and Oceanic Sciences, McGill University, Montreal, and Recheche en Prévision Numérique, Meteorological Service of Canada, Dorval, Quebec, Canada
[3]Department of Atmospheric and Oceanic Sciences, McGill University, Montreal, Quebec, Canada

1. INTRODUCTION AND MOTIVATION

*A new triple-moment bulk microphysics scheme (BMP) described in Milbrandt and Yau (2005b, hereafter MY#, where # is the number of moments predicted) has been implemented in the Advanced Regional Prediction System (ARPS; Xue et al. 2003). The scheme predicts up to three moments of the size distribution for 2 categories of liquid (cloud droplets and raindrops) and 4 categories of precipitating ice (ice crystals, snow, graupel, and hail). Prognostic equations for the mixing ratio, number concentration, and radar reflectivity factor are provided for each cloud and hydrometeor category except cloud water, for which reflectivity is not predicted. The size distribution for each precipitating category is assumed to be of the form,

$$N(D) = N_0 D^{\alpha} e^{-\lambda D} \quad (1)$$

where the full 3-moment version of the scheme allows the intercept (N_0), slope (λ), and shape (α) parameters of the distribution to vary independently. The number concentration, mixing ratio, and radar reflectivity factor are proportional to the 0th, 3rd, and 6th moment of the size distribution, respectively.

In this study, we apply the scheme in its 1, 2, and 3-moment modes to simulations of the 3 May 1999 Oklahoma tornadic supercells (see *Fig. **1***). The motivation for this study comes from the experience that many numerical simulations of intense convection in typical continental environments of high CAPE produce cold pools that are too large and intense, when typical single-moment microphysics schemes (mostly using an exponential size distribution) are used with typical fixed values for the intercept parameter N_0. Further motivation comes from past work (e.g., Gilmore et al. 2004, Snook and Xue 2006, Milbrandt and Yau 2006a,b) in which significant differences (in some cases factor of 2 or more differences in total precipitation, for example), in many storm characteristics were seen when varying the uncertain size distribution parameters such as the intercept. It is hypothesized that allowing more parameters of the various hydrometeor size distributions to vary independently in time and space, as a multi-moment scheme does, may improve the overall simulation of convective storms with much less "tuning" of the parameters necessary. Such parameters are effectively predicted in multi-moment schemes.

In addition to the multi-moment scheme, we examine the impact of using a modified version of the WRF Single Moment Microphysics scheme (WSM6), wherein the intercept parameter for rain is diagnosed as a function of liquid water content (Zhang et al. 2007), and compare these results with those from the original, fixed-intercept version of the WSM6 scheme.

In the 3 May 1999 case, several long-track, and in some cases violently tornadic supercells tracked across much of central OK, with available data suggesting small and relatively weak cold pools (see *Fig. **1***). The storms were noteworthy for producing over 70 tornadoes in Oklahoma alone, including the deadly F5 tornado that struck parts of Moore, OK and southern Oklahoma City. Real-data simulations of the event using the aforementioned single-moment schemes with the ARPS produce fewer organized storms due in large part to large and expansive cold pools depriving much of the domain of surface based instability. We seek to determine the underlying causes for this bias, and to examine the impact of predicting two or more moments of the size distribution, where allowing the number concentration (and thus the intercept parameter) to vary independently may allow for much less arbitrariness over pre-specifying the values of these parameters. Further, the impact of model horizontal resolution is examined and the dependency of microphysics impact on grid resolution is also assessed.

2. METHODOLOGY

Simulations were performed for this event using the nonhydrostatic ARPS model. Initial conditions for the real-data simulations were produced using the ARPS Data Analysis System (ADAS), which uses an iterative successive correction scheme that converges to the optimal interpolation (OI) solution (e.g., Brewster 1993, Case et al.. 2002, Lazarus et al.. 2002). The ADAS includes a complex cloud analysis scheme that utilizes satellite and radar observations to adjust the initial state of the model on convective scales (Zhang et al. 1998; Zhang 1999; Brewster 2001a,b; Hu et al. 2006).

* *Corresponding author address:* Daniel T. Dawson II, CAPS/SoM, National Weather Center, Suite 5900,120 David Boren Blvd, Norman OK 73072, USA; ddawson@ou.edu

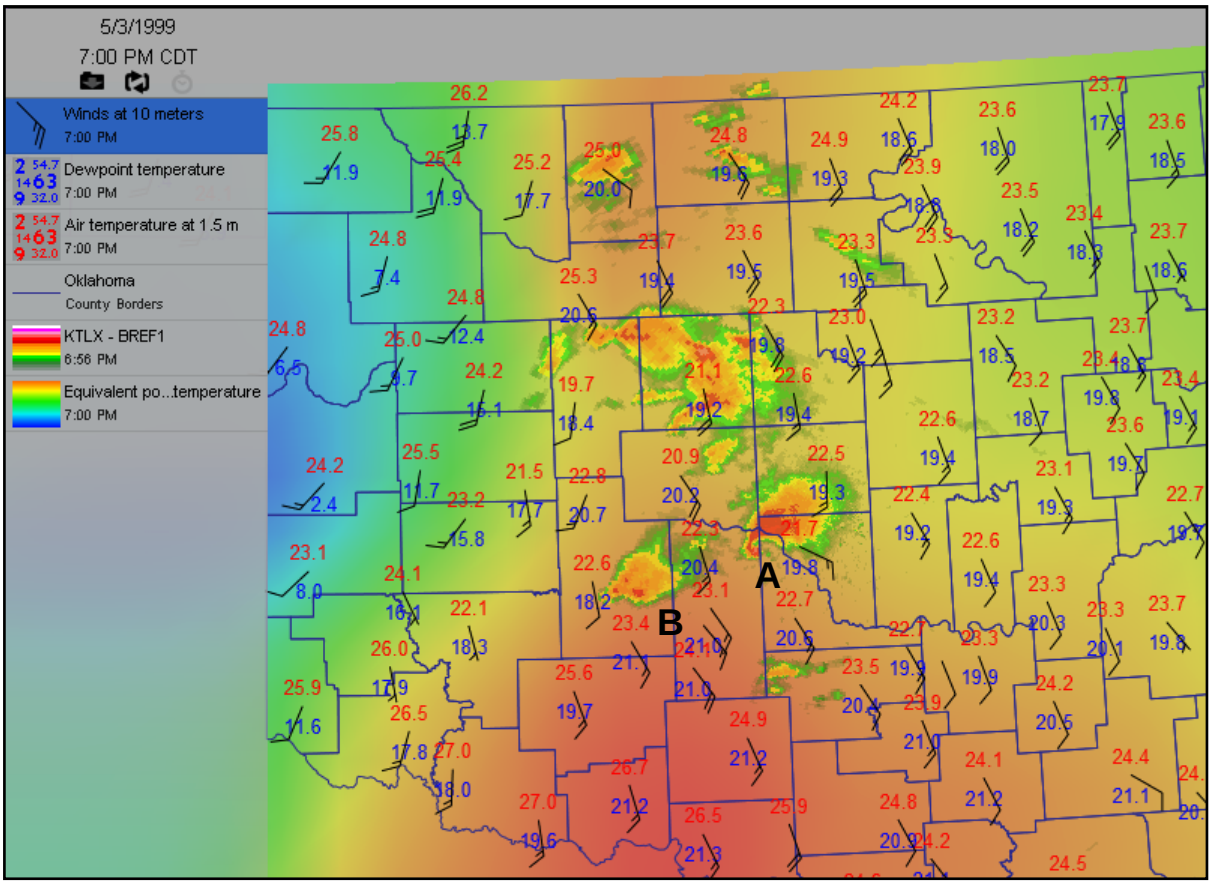

Fig. 1. Observed surface conditions and radar reflectivity at 0000 UTC 4 May 1999 in Oklahoma, by the Oklahoma Mesonet. Shown are base reflectivity from KTLX, mesonet stations with observed wind direction, speed, and 2 m air and dewpoint temperature, and color-shaded equivalent potential temperature.

The real-data simulations were performed at a horizontal grid spacing of 3 km (see *Fig.* ***2***), and were run with full physics, including surface and radiation physics (Xue et al. 2001). The dimensions of the 3 km grid were 1440×1440×20 km^3. Vertical grid stretching was employed in all simulations using 53 vertical levels starting with 20 m grid spacing at the low levels. Analysis background and lateral boundary conditions came from the North American Regional Reanalysis (NARR) at 3 hour intervals, interpolated to the 3 km analysis grid. Fifteen-minute assimilation cycles were performed over a 1-hour period from 2100 to 2200 UTC, wherein radar data from the Oklahoma City WSR-88D radar (KTLX) was assimilated via the cloud analysis at 15 minute intervals. This captured some of the early stages of development of the two initial supercell thunderstorms that formed that afternoon. These can be seen in *Fig.* ***1*** as the two storms marked as A and B. Storm A started to spawn tornadoes at 1641 UTC. The ADAS analyses at 2100 and 2200 UTC also included conventional surface and upper air data. The Oklahoma Mesonet data were included. A forecast cycle was then run from 22Z 3 May 1999 out to 7 hours. A total of 7 microphysics schemes and/or configurations were tested, including two versions of the Lin (Lin e al. 1983, Tao and Simpson 1993) scheme, the WRF single-moment (WSM6) 6-category scheme (Hong et al. 2006) and its modified version using diagnostic intercept parameter for rain (Zhang et al. 2007), and the 1, 2 and 3-moment versions of the Milbrandt-Yau scheme (MY1, MY2, and MY3, Milbrandt and Yau 2005a,b) These are listed in Table 1, and all simulations are identical except for the microphysics configuration.

To further examine the impact of microphysics at higher resolutions that some recent work suggests are crucial to properly resolving convection (e.g., Bryan et al. 2003), a series of simulations at 1 km, 500 m, 250 m, and 100 m horizontal grid spacings were performed. A smaller subset of the microphysics configurations were tested in these simulations: the default ARPS Lin scheme, and the MY1, MY2, and MY3 schemes. Rather than directly increasing the real data simulations which is very expensive, a sounding was extracted from the real-data simulations that was subjectively determined to be representative of the unstable inflow region of the model storms and used in idealized single-sounding simulations. This extracted sounding has many similarities to the observed Norman Oklahoma 0000 UTC 4 May 1999 sounding (see *Fig.* ***3***), especially in the kinematics. Thermodynamically, the main differences

between the two are the lack of a significant cap and somewhat weaker mid-level lapse rates in the extracted sounding. The cap in the observed sounding may be due to low-level cooling due in turn to anvil shading from the approaching supercell storm at the time the sounding was taken. The large CAPE difference between the two soundings is due partly to the cooler surface temperatures in the observed sounding, as well as the fact that the observed sounding was truncated in the upper levels so that a full CAPE calculation is not possible. Because of these reasons, and the fact that the idealized simulations contain no mesoscale forcing mechanisms to maintain convection in the presence of such a large cap, the observed sounding was not suitable for use directly to initialize the storm environment in the model simulations. For this reason, the extracted sounding was used instead to define the storm environment on a 128x175x20 km^3 grid. Convection was initiated with an ellipsoidal thermal bubble of maximum potential temperature perturbation of 4 K with a horizontal radius of 10 km and vertical radius of 1.5 km, centered 1.5 km above ground, and 35 and 25 km from the left and south edge of the domain, respectively. The simulations were run out to 2 hours. The idealized simulations did not contain radiative forcing or surface fluxes, with our main purpose being to isolate the direct effects of variations in microphysics. While the absence of surface friction may affect the cold pool propagation somewhat, its inclusion tends to modify the environmental sounding over time, an undesirable result for the purposes of these simulations.

The large sizes of these computational grids require the use of a large number of processors. The ARPS was used in the distributed-memory parallel mode via MPI.

3. RESULTS

3.1 Real-data 3 km simulations

Mostly preliminary, qualitative results will presented in this paper. A budget analysis of the various microphysical processes contributing to heating and cooling in the context of cold pool production is in progress and will be presented in future papers. Fig. 4 shows the surface reflectivity and contours of water vapor mixing ratio and Fig. 5 the surface temperature fields, for each of the 7 real-data simulations at a forecast time of 2 hours, valid at 0000 UTC 4 May 19. Fig. 6 shows the corresponding surface dewpoint fields. All simulations overpredict cold pool strength and area, particularly in regards to moisture fields. However, significant differences are seen between the simulations, with the two WSM6 schemes showing the largest and strongest cold pools, while the Lin with reduced N_{0r}, default Lin, MY2, and MY3 schemes show similar and somewhat weaker cold pool strengths than the WSM6 schemes. However, in regard to reflectivity, the MY2 and MY3 schemes show the most realistic reflectivity structure and intensity of all the schemes, particularly in the hook echo and forward flank regions of the modeled supercells compared to the observation (cf. Fig. 1). A vertical east-west cross section of equivalent potential temperature through the leading supercell of the Lin simulation at 0000 UTC is shown in ***Fig. 7***. From this cross section and similar ones from the other simulations (not shown), it is clear that the dry air present in the surface cold pools comes primarily from the mid-troposphere that is brought downward in large convective downdrafts more or less undiluted. Causes of the strong cold pool in the model and the reasons why this is not observed is currently being investigated. Microphysics deficiencies and inadequate treatment of subgrid-scale turbulence processes that can cause strong entrainment/detrainment and mixing are some of the likely culprits, with the latter closely related to model resolution. The dependency of results on model resolution is examined next.

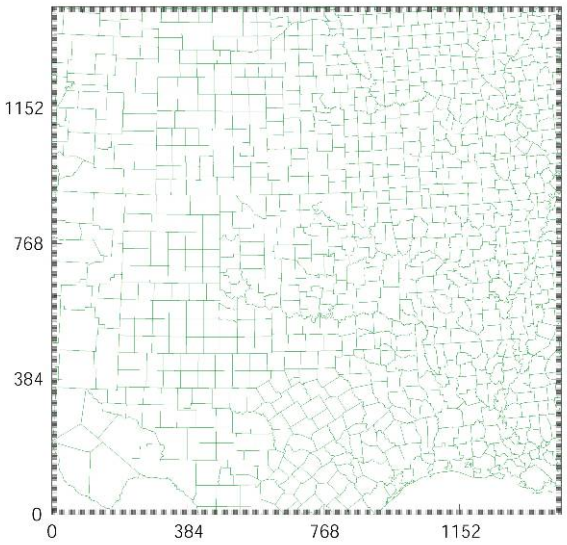

Fig. 2. Computational domain for the 3 km real-data simulations.

Table 1. Microphysics configurations in the 3 km real-data simulations

Microphysics scheme/configuration	Description
LIN	Based on Tao and Simpson (1993)
LINRN0R	Lin scheme with N_{0r} reduced from default value of 8.0×10^6 m^{-4} to 4.0×10^5 m^{-4}
WSM6	WRF Single-moment 3-class ice scheme (Hong et al. 2006)
WSM6DN0R	Modified WSM6 with diagnostic N_{0r} as a function of rainwater content
MY1	Single-moment version of the MY scheme
MY2	Double-moment version of the MY scheme
MY3	Triple-moment version of the MY scheme

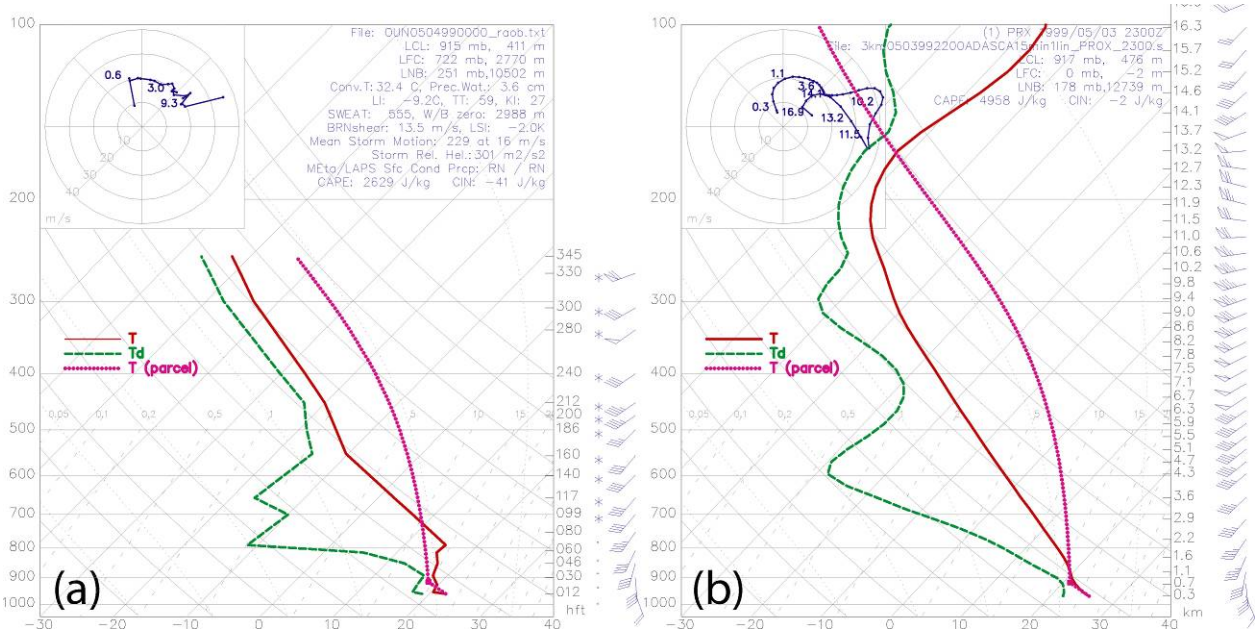

Fig. 3. (a) Observed 0000 UTC 4 May 1999 sounding at Norman Oklahoma (KOUN), (b) extracted sounding at 2300 UTC from the inflow region of the model storms in the 3 km real-data simulation with Lin scheme.

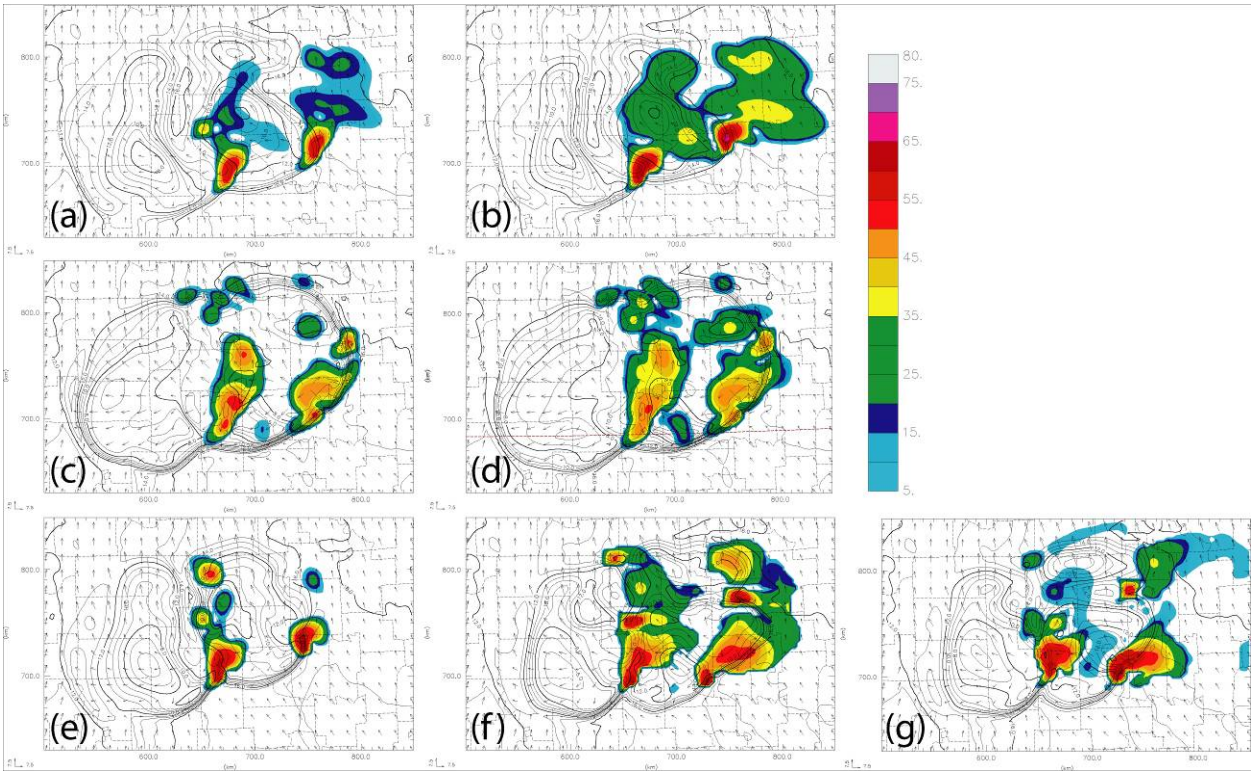

Fig. 4. Surface reflectivity, water vapor mixing ratio (black contours in 1 g/kg increments), and surface wind vectors at 2 hours (0000 UTC 4 May 1999) for the 3km real-data simulations: (a) LIN, (b) LINRN0R, (c) WSM6, (d) WSM6DN0R, (e) MY1, (f) MY2, (g) MY3.

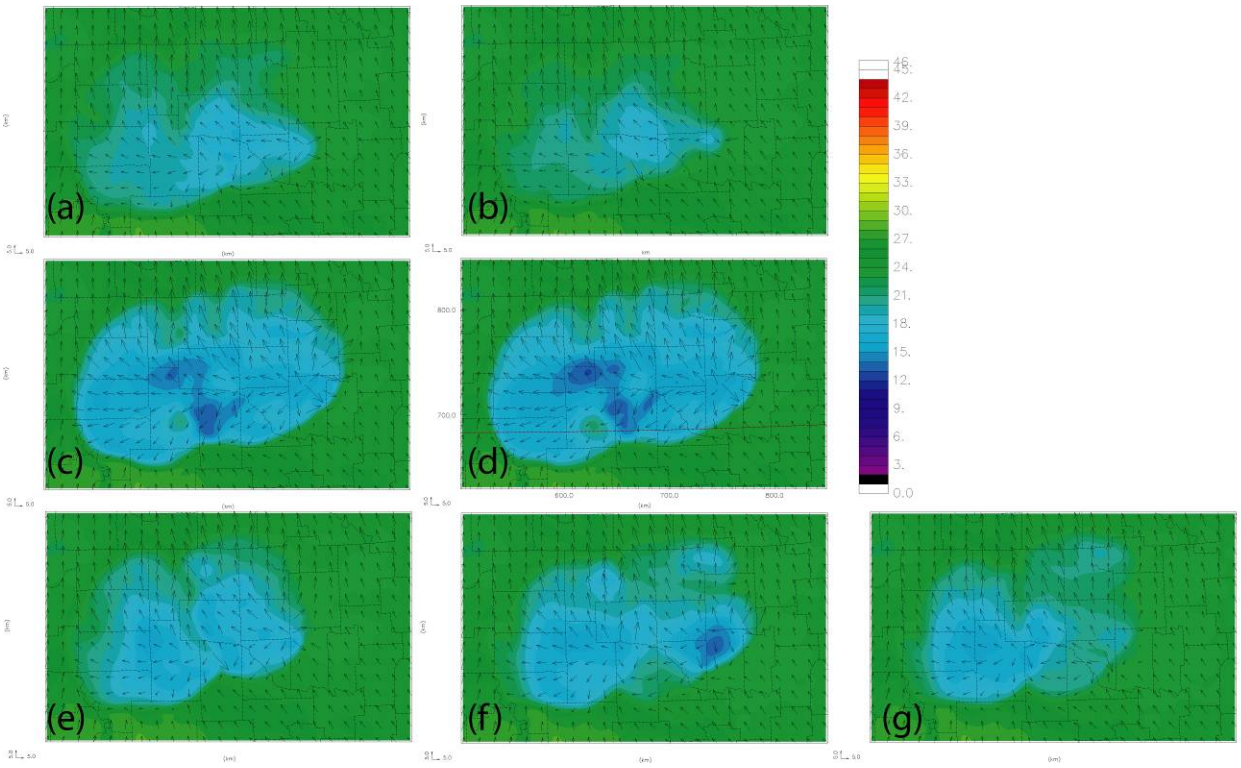

Fig. 5. As in Fig. 4 but for color contours of surface temperature.

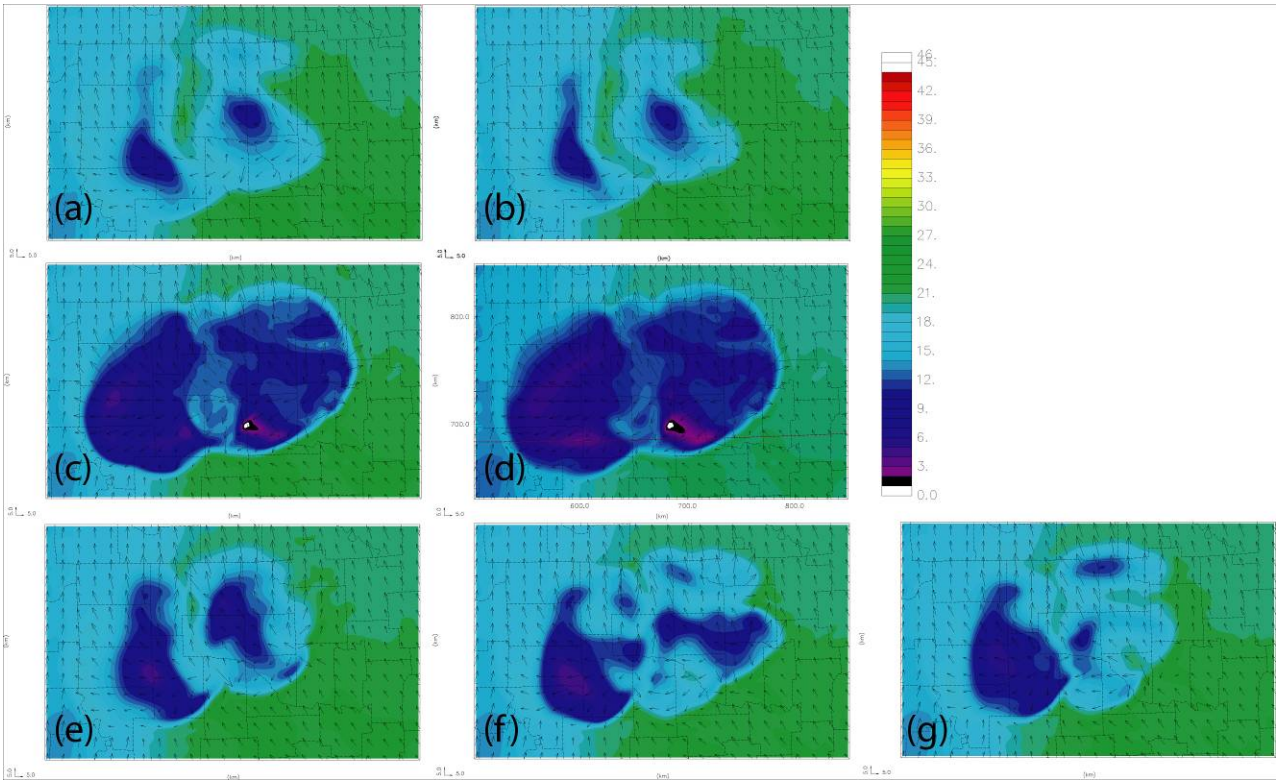

Fig. 6. As in Fig. 4 but for color contours of dewpoint temperature.

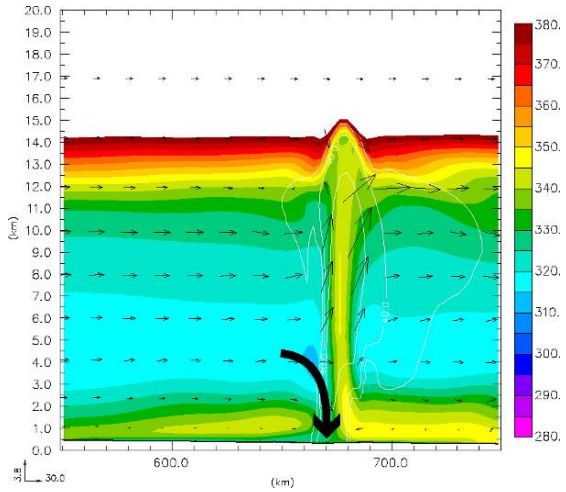

Fig. 7 Vertical east-west cross section through the location of the maximum updraft at 0000 UTC 4 May 1999. Shown are color-shaded contours of equivalent potential temperature, and contours of reflectivity (white) in 20 dbZ increments.

3.2 High-resolution idealized simulations

In the 1 km single-sounding simulations, the initial storm decayed by less than 1 hr and sustained convection could not be maintained; the results are therefore not shown here. However, the early stages of the initial storm development showed a more rapid development of the cold pool with the Lin and MY1 schemes than in the MY2 and MY3 schemes. The 500 m simulations (***Fig. 8***) featured a storm that lasted through most of the 2 hr integration period in the double and triple-moment cases, while the storm began to decay after 1 hr with the Lin and MY1 schemes. In these cases, the differences in cold pool strength between the single and double-moment simulations are dramatic. The reflectivity structure also shows a much better developed forward flank region in the 2 and 3-moment simulations, which is comparable in shape, and orientation to the forward flank region of the observed storms (cf. *Fig.* ***1***). However, the size of the forward flank appears somewhat overpredicted in the 2 and 3-moment simulations (60-70 km long in the east-west direction, as compared to 40-50 km long in the observed storms), while it was underpredicted (20-30 km long) in the single-moment simulations. Finally, results of 250 m and 100 m simulations (not shown) comparing the Lin scheme and the MY2 scheme show overall very similar results to the 500 m simulations. This suggests that much of the benefit, which includes much more realistic weaker cold pools and better reflectivity structures, of moving to a double moment microphysics scheme, at least for this case, may be reaped at horizontal resolutions approaching 500 m. Moreover, as Fig. 8 suggests, most of the reduction in cold pool strength and improvement in reflectivity structure arguably comes from moving from 1 to 2 moments and the impact going from 2 to 3 moments is smaller. However, given the idealized and preliminary nature of these sets of simulations, more work needs to be done to determine if these results extend to a real-data framework within a horizontally inhomogeneous environment. Detailed diagnostic and budget analyses on the microphysical processes are also being performed to fully understand the reasons for the key differences.

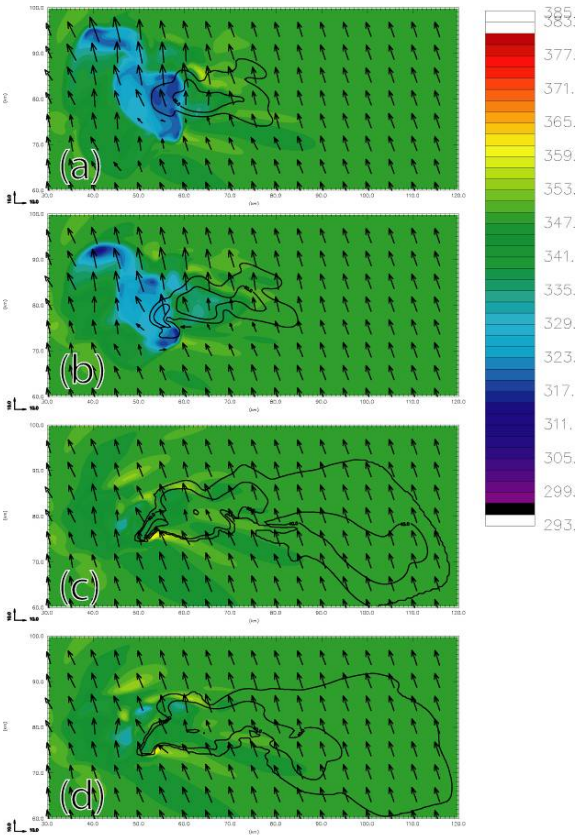

Fig. 8. Equivalent potential temperature (color contours), surface reflectivity (increments of 20 dbZ, starting at 20 dbZ), and surface wind vectors for (a) LIN, (b) MY1, (c) MY2, and (d) MY3 at 1 hour of the 500 m single-sounding simulations.

4. SUMMARY AND FUTURE WORK

In this paper, we have presented preliminary results from a series of numerical simulations of the 3 May 1999 Oklahoma tornadic supercell storms, in which the impact of different microphysics schemes and formulations were tested. In particular, the impact of predicting more than one moment of the size distribution (in either exponential or gamma form) for the various hydrometeor categories was examined. Preliminary results indicate that the impact on the cold pool strength is resolution-dependent, and becomes most dramatic at horizontal grid spacings smaller than 1 km, although

subtle improvements in the reflectivity structure of the simulated storms is seen even at the relatively coarse 3 km grid spacing. Further, most of the improvement appears to come when moving from predicting a single moment (in which the intercept parameter is fixed (or possibly diagnosed for some categories) to predicting in addition the total number concentration (allowing the intercept parameter to vary independently in time and space).

A detailed analysis, including a full budget analysis of the microphysical processes contributing to heating and cooling in the context of cold pool production (i.e. rain evaporation, melting and sublimation of ice categories, and collection of liquid by ice), is underway and the results will be presented in future papers.

Future work will expand into nested-grid real-data simulations at 500 m or smaller grid spacings to determine if the results of the idealized simulations hold for more realistic settings. Attention will also be given to the problem of initializing multiple moments from radar data in our complex cloud analysis procedure. We also plan to investigate very high-resolution nested simulations (100 m or smaller grid spacing) of the main tornadic supercell (in this case the one that produced the Moore, OK F5 tornado) to determine the impact of the multi-moment microphysics on the prediction and simulation of tornadoes within the storms. Finally, extensions to other cases are planned, including the 9 May 2003 OKC tornadic storm, and the 20 March 2006 Cold-core tornadic storms.

ACKNOWLEDGEMENTS This work was mainly supported by NSF Grant ATM-0530814, and by the National Science Foundation Graduate Research Fellowship awarded to the first author. The authors would like to thank OSCER and the Pittsburgh Supercomputing Center for the use of their supercomputing facilities. Mr. Yunheng Wang is acknowledged for initial implementation of the multi-moment scheme within ARPS.

6. REFERENCES

Brewster, K., 1996: Application of a Bratseth analysis scheme including Doppler radar data. Preprints, 15th Conf. Wea. Anal. Forecasting, Norfolk, VA, Amer. Meteor. Soc., 92-95.

——, 2001: Phase-correcting data assimilation and application to storm-scale numerical weather prediction. Part I: Method description and simulation testing. *Mon. Wea. Rev.*, **131,** 480-492.

——, 2001: Phase-correcting data assimilation and application to storm scale numerical weather prediction. Part II: Application to a Severe Storm Outreak. *Mon. Wea. Rev.*, **131,** 493-507.

Bryan, G. H., J. C. Wyngaard, and J. M. Fritsch, 2003: Resolution requirements for the simulation of deep moist convection. *Mon. Wea. Rev.*, **131**, 2394-2416.

Case, J. L., J. Manobianco, T. D. Oram, T. Garner, P. F. Blottman, and S. M. Spratt, 2002: Local Data Integration over East-Central Florida Using the ARPS Data Analysis System. *Wea. Forecasting*, **17,** 3-26.

Gilmore, M. S., J. M. Straka, and E. N. Rasmussen,2004: Precipitation uncertainty due to variations in precipitation particle parameters within a simple microphysics scheme. *Mon.Wea. Rev.*, **132,** 2610-2627.

Hong, S.-Y. and J.-O. J. Lim, 2006: The WRF singlemoment 6-class microphysics scheme (WSM6). *J. Korean Meteor. Soc.*, **42,** 129-151.

Hu, M., M. Xue, and K. Brewster, 2006: 3DVAR and cloud analysis with WSR-88D level-II data for the prediction of Fort Worth tornadic thunderstorms. Part I: Cloud analysis and its impact. Mon. Wea. Rev., 134, 675-698.

Lazarus, Steven M., Ciliberti, Carol M., Horel, John D., Brewster, Keith A. 2002: Near-Real-Time Applications of a Mesoscale Analysis System to Complex Terrain. *Weather and Forecasting*: Vol. 17, No. 5, pp. 971–1000.

Snook, N., and M. Xue, 2006: Sensitivity of tornadogenesis in very-high resolution numerical simulations to variations in model microphysical parameters. Extended Abstract, 23rd Conf. on Severe Local Storms, St. Louis, MO., Amer Met. Soc.

Tao, W.-K. and J. Simpson, 1993: Goddard cumulus ensemble model. Part I: Model description. *Terres. Atmos. Ocean Sci.*, **4,** 35-72.

Milbrandt, J., and M.K. Yau, 2005: A multi-moment bulk microphysics parameterization. Part II: A proposed three-moment closure and scheme description. *J. Atmos. Sci.* , **62**, 3065-3081.

——, 2006: A multimoment bulk microphysics parameterization. Part III: Control simulation of a hailstorm. *J. Atmos. Sci.*, **63**, 3114-3136.

——, 2006: A multimoment bulk microphysics parameterization. Part IV: Sensitivity experiments. *J. Atmos. Sci.*, **63**, 3137-3159.

Xue, M., coauthors, 2001: The Advanced Regional Prediction System (ARPS) - A multiscale nonhydrostatic atmospheric simulation and prediction tool. Part II: Model physics and applications. Meteor. Atmos. Phy., 76, 143-165.

——, D.-H. Wang, J.-D. Gao, K. Brewster, and K. K. Droegemeier, 2003: The Advanced Regional Prediction System (ARPS), storm-scale numerical weather prediction and data assimilation. *Meteor. Atmos. Physics*, **82,** 139-170.

Zhang, G., M. Xue, Q. Cao, and D. Dawson, 2007: Diagnosing the intercept parameter for exponential raindrop size distribution based on video disdrometer observations. Geophys. Res. Letters, Under review.

Zhang, J., F. Carr, and K. Brewster, 1998: ADAS cloud analysis. *Preprints, 12th Conf. on Num. Wea. Pred.*, Phoenix, AZ., Amer. Met. Soc., 185-188.

——, 1999: Moisture and Diabatic Initialization Based on Radar and Satellite Observation, School of Meteorology, University of Oklahoma, 194 pp, [Available from School of Meteorology, University of Oklahoma, Norman OK 73019].